Monitoring Geothermal Power Plant Turbine Movement in Steam

Ye Lingzhu
Electrical & Computer Engineering, NUS
U0607202@nus.edu.sg

***Abstract*—This Agilent Engineering Excellence Project was aimed to use Data Acquisition (DAQ) system (U2353A USB module) and Agilent VEE Pro to monitor geothermal plant turbine movement from steam. In this project, a geothermal power plant demonstration model and a real-time monitoring system were built successfully. The demonstration model was constructed by a steam engine and several sensors. These sensors can capture the temperature, pressure in steam, the speed of turbine (flywheel in this project), the output voltage of electrical power generator and the environmental noise level. Those data were captured and transferred to the computer through U2353A. At the same time, a GUI was designed and programmed by utilizing Agilent VEE Pro. The monitoring system collects readings from U2353A and displays them on the user interface. Compared with the conventional approaches, this model is able to provide reliable data and to facilitate the future research. Through the process, many theories in the real industry were verified.**

I. Introduction

THE usage of geothermal energy to generate electricity was firstly began in 1904 in the Tuscany village of Larderello when Prince Piero Ginori Conti hooked a 3/4-hp reciprocating engine to a steam pipeline, thereby driving a small generator. The worldwide geothermal industry grew rapidly in the 1970s and 1980s, driven strongly by the oil shocks of 1973 and 1979 and the push to develop alternative renewable sources of energy. The state of the technology has advanced significantly such that an extensive menu of energy conversion system is available to match the highly variable physical and chemical characteristics of geothermal resources found around the world.[1]

Electricity is produced by geothermal in 24 countries, five of which obtain 15-22% of their national electricity production from geothermal energy. Direct application of geothermal energy (for heating, bathing etc.) has been reported by 72 countries. By the end of 2004, the worldwide use of geothermal energy was 57 TWh/yr of electricity and 76 TWh/yr for direct use. Ten developing countries are among the top fifteen countries in geothermal electricity production. Six developing countries are among the top fifteen countries reporting direct use. [2]

The largest group of geothermal power plants in the world is located at The Geysers, a geothermal field in California, United States. [3] Singapore has three hot springs can be used. It has already been considered as an attractive geothermal energy exploration target [4].

There are three different types of geothermal power plants: dry steam plants, flash steam plants, and binary cycle plants.

When a geothermal power plant uses steam in the same form as it comes from the ground, the plant is called a dry steam plant. Steam reaching temperatures of 150 °C or more is then brought up to the surface. Once the steam reaches the turbines, it spins the turbine blades.

In flash steam geothermal power plants, water is pumped from the reservoir under high pressure. The pressure keeps the water in a liquid state even though the water's temperature is well above the boiling point. Once it reaches the surface, the pressure is relieved and water greater than 182 °C flashes into steam. The steam is then used to turn the turbine blades.

Binary cycle geothermal power plants do not use water to turn the turbine blades. Rather, water with temperatures between 107.2-182.2 °C is used to heat a separate fluid that has a boiling point well below that of water. When this fluid is vaporized, the vapour is used to turn the turbine blades. [5]

The first two types of geothermal power plant are more commonly used. They are easy to develop and the technology is relative mature. Like all steam turbine generators, the force of steam is used to spin the turbine blades which spin the generator, producing electricity. The saturated steam in use can be divide into wet steam type and dry steam type. The latter has high efficiency to generate electricity because it skips the vapour-water separation step. The geothermal turbine blades have several layers with different design. They are driven by the steam in different phases with different temperature and pressure. It maximize the use of thermal energy.

This project is aimed on two major tasks: to build a demonstration model of geothermal power plant (hardware system) and to develop a real-time monitoring of power plant (software system). Due to technical limitation, the demonstration model was built base on the principle of dry steam plant. It will direct use the steam generated to spin a single layer of turbine blades. Then generate electricity.

II. Hardware System Design

A. Demonstration Model Design

The hardware of measurement system includes two parts: the demonstration model and several sensors. The early demonstration model was simply designed. An induction cooker was a substitute for geothermal generator, while a boiling pot was used to generate steam in order to drive the fan which represents turbines. Due to the poor closeness of the whole system, both the temperature and pressure of the steam were not high enough. Thus, the steam could not provide enough power for the measurement system.

Besides monitoring the temperature and pressure of the steam, the original idea to estimate the power of steam was realized by measuring the rotation speed of the fan which was fixed on the rotor of a motor. During the experiments, by

observing the relationship between fan speed and output voltage of the motor, a formula to calculate the rotation velocity was able to be generated. However, though the steam was powerful enough to drive the fan individually, it couldn't drive it together with the motor due to the big inertia. In practice, the output voltage of the motor was nearly zero. An anemometer was used to measure and verify the steam velocity. The anemometer and vane probe were shown below. From the testing, the velocity was around 2m/s, which was really low.

One way to increase the power of steam was to increase its temperature. It could be achieved by adding solute to increase the boiling point of water. Sugar, salt and monosodium glutamate (MSG) were added. Compare the results, salt was the best choice which can improve the boiling point up to 110 centigrade degree (during saturation). However, the power of the hotter steam was still not enough to drive the fan. Also, the plastic fan started to melt in the hot steam when the temperature kept increasing. This attempt was unsuccessful. In order to make the measurement of the project more accurate and practical, a Wilesco D 16 toy steam engine had been purchased as the demonstration model of a geothermal power plant.

Wilesco D 16 toy steam engine with mirror polished and nickel plated boiler, diameter 2.25 in, length 5.5 in, boiler capacity 15 cubic inches, with water gauge glass. Double action reversible brass cylinder with flywheel, spring loaded safety valve, additional steam whistle with chain, steam regulator, flywheel of 3.25 in diameter with grooved pulley, sturdy attractive die cast piston rods, centrifugal governor, steam jet oiler and railing. The condensed water is fed to a tank, hidden behind the boiler house, causing the chimney to smoke realistically. The size of finely painted metal base plate is W9.75 in x L12.25 in x H 11.0 in (including smoke stack), and weight, 3 lbs. 10oz.

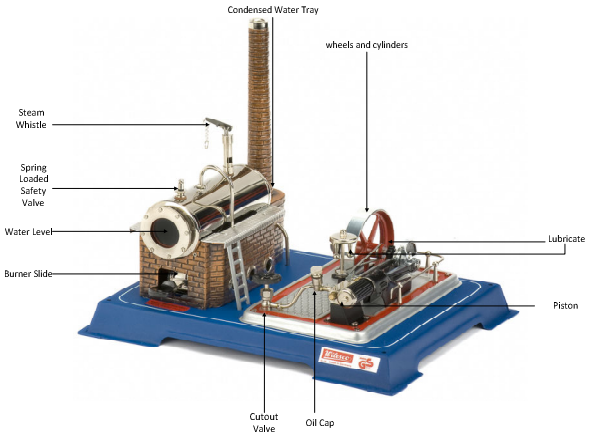

Fig. 1. Wilesco D 16 toy steam engine

In the monitoring system, the following sensors would be designed and applied on the demonstration model. And the analog input pins on U2353A data acquisition system were listed at the back.

- Temperature Sensor (Pin3,@103)
- Pressure Sensor (Pin4,@104)
- Rotation Speed Sensor(Pin1,@101)
- Noise Sensor (Pin6,@105)
- DC Generator (Pin2,@102)

B. *Temperature Monitoring*

Precision Centigrade Temperature Sensors LM35DZ was chosen to monitor the internal temperature of the boiler. It is a precision integrated-circuit temperature sensor, whose output voltage is linearly proportional to the Celsius (Centigrade) temperature. It thus has an advantage over linear temperature sensors calibrated in °Celsius, which is +10.0mV/°C scale factor. The LM35 does not require any external calibration or trimming to provide typical accuracies of ±1⁄4°C at room temperature and ±3⁄4°C over a full −55 to +150°C temperature range. Low cost is assured by trimming and calibration at the wafer level. The LM35's low output impedance, linear output, and precise inherent calibration make interfacing to readout or control circuitry especially easy. It can be used with single power supplies, or with plus and minus supplies. The package is shown below.

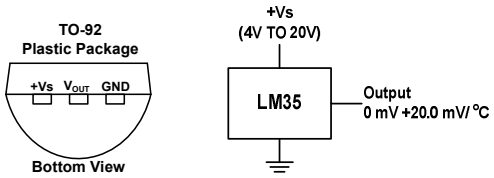

Fig. 2. Temperature sensor LM35DZ and application circuit

There are three thermo-points on the geothermal plant could be monitored: the internal temperature of the boiler, the temperature near piston (turbine) and the temperature of exhaust gas. By comparing the temperatures of the three points, the heat efficiency can be calculated. These results could be used to design the utility of heat in exhaust steam. In this project, the point in the boiler was specially focused.

Holes might need to be drilled on the boiler and pipes to put sensors in. But drill holes may create high probability to destroy the closeness of the whole system. Accurate temperature and pressure measurements are vital to the understanding of steam turbine efficiency, reliability, and service condition. Hence, an alternative method was designed to avoid the problem. A housing was designed and lathed to place the sensors inside it. Then mount the housing on the boiler in order to get the parameters inside. It was made of brass to avoid rust. The AutoCAD drawing is shown as follows.

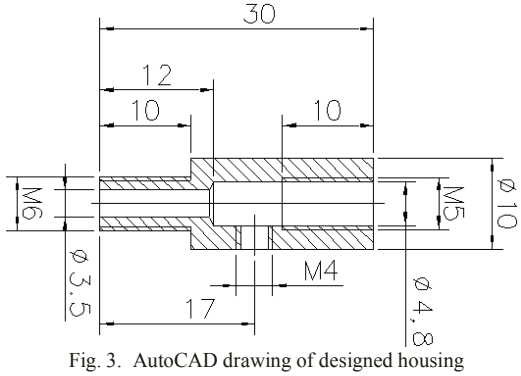

Fig. 3. AutoCAD drawing of designed housing

C. *Pressure Monitoring*

To monitor the pressure precisely is closely linked to safety operation. Because it was hard to predict the pressure range of steam in the boiler, a pre-measurement was applied before choose the pressure sensor. The pressure in the boiler measured by a pressure gauge was around 1.54 bar. Hence, the pressure range can be chosen within 10-250 kPa.

After comparing various sensors, MPX4250AP pressure sensor was chosen to apply in the system. MPX4250A series Manifold Absolute Pressure (MAP) sensor for engine control is designed to sense absolute air pressure within the intake manifold. This measurement can be used to compute the amount of steam required for each cylinder. The series of piezoresistive transducer is a state-of-the-art monolithic silicon pressure sensor designed for a wide range of applications, particularly those employing a microcontroller or microprocessor with A/D inputs. This transducer combines advanced micromachining techniques, thin-film metallization and bipolar processing to provide an accurate, high-level analog output signal that is proportional to the applied pressure. The small form factor and high reliability of on-chip integration make the free scale sensor a logical and economical choice for the automotive system engineer.

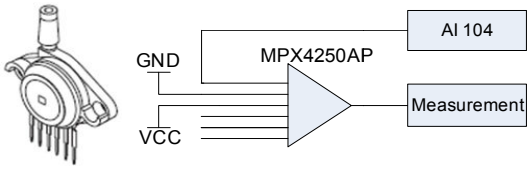

Fig. 4. Pressure sensor MPX4250A and application circuit

For an accurate testing of the internal pressure in the boiler, the steam whistle on the boiler would be replaced by the housing which was introduced in the early part. And the pressure sensor would be directly mounted on the housing.

D. *Rotation Speed Monitoring*

The initial idea to measure the speed of fan/blade was to fix it on the rotor of a motor. If the relationship between the output voltage of the motor and rotation speed can be obtained, the rotation speed could be got by monitoring the output voltage. However, it is hard to find the proper relationship. After several attempts, a rotational sensor KMI15/16 was chosen at first. It is a magneto-resistive sensor module with an integrated signal conditioning electronics to provide a simple and cost effective solution for rotational speed measurements. The output signal will be larger than using the Hall-effect sensor. This sensor can perform very well if it is used together with the gears. However, for the model in this project, it needs to be applied on the flywheel (substitute of turbine). Since the flywheel is an inertia wheel, if paste the magnetic disc on the surface of the wheel, it might destruct the balance. Besides, the magnetic sensor may not be sensitive enough to collect data from the wheel if the piston runs very fast. This may affect the accuracy of the measurement.

Under the given conditions, a Reflective Optical Sensor with Transistor Output—TCRT5000 was finally put into use. The TCRT5000 (L) has a compact construction where the emitting-light source and the detector are arranged in the same direction to sense the presence of an object by using the reflective IR beam from the object. The operating wavelength is 950 mm. The detector consists of a phototransistor.

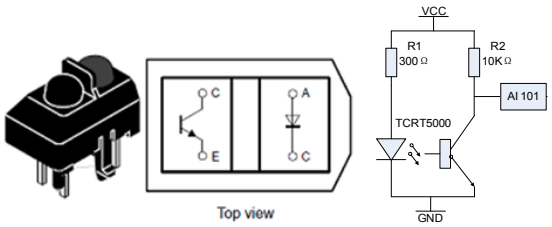

Fig. 5. Reflective optical sensor TCRT5000 and application circuit

E. *Generator*

The basic function of a geothermal power plant is to generate electricity. Thus, part of the demonstration model was designed to be the electrical generator. Because the efficiency of this model was quite low, a 5v DC motor was used as the electrical generator. And a LED array was used to demonstration the results. LTA-1000 series bar graph array was chosen to demonstrate the electricity generated by the dc motor. The LTA-1000 series are ten rectangular light sources array displays designed for a variety of applications. The package picture is shown below.

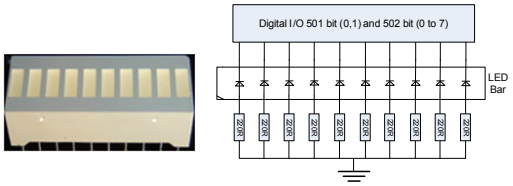

Fig. 6. LED array LTA-1000 and connection circuit

F. *Noise Level Monitoring*

In the real industry, the noise level around a power plant needs to be controlled within certain level. An acoustical site evaluation for a power plant was conducted by Navcon Engineering. The major noise sources include inlet, generators, gearbox, and turbine and exhaust stake, etc. The emission levels of these sources were provided by the equipment manufactures. The noise levels were computed at the property line and over a calculation area. Figure 7. shows the noise scenario with the additional noise control. It presents the predicted noise levels in terms of noise contour lines and sound level charts at point receivers.[7]

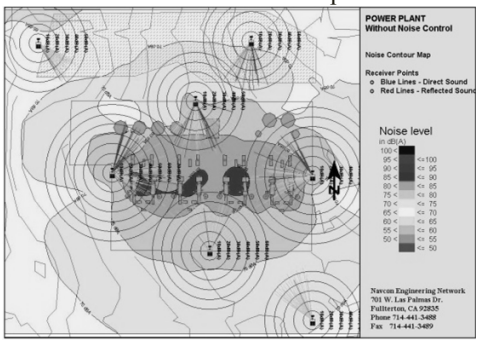

Fig. 7. Noise scenario with the additional noise control

In this project, the sensor chosen is major used to detect the noise level of the flywheel and piston part. The amplified 'Mini' Sisonic Microphone (SPM0103ND3) applied to the system.

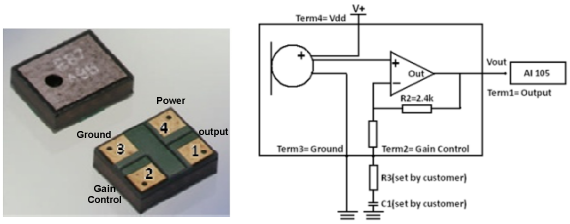

Fig. 8. Mini microphone SPM0103ND3 and application circuit

III. VEE PRO PROGRAMMING

In this project, the version of VEE Pro is 9.0. Agilent VEE Pro 9.0 is an easy-to-use graphical language environment which provides a quick path to measurement and analysis. Designed for easy expansion, flexibility and compatibility with the latest industry standards, Agilent VEE allows seamless operation with hardware and software from Agilent and other manufacturers.[6]

A. Temperature Monitoring

The output signal from LM35 is analog signal. It could use analog input pin of U2353A to transfer data into computer. Then the output voltage needs to be converted to Celsius degree for displaying on the user interface. Meanwhile, according to the data sheet of LM35DZ, the output voltage and temperature at that point has the follow relationship:

- +1500mV at +150°C
- +250mV at +25°C
- -550mV at +55°C

The linear scale factor has also been described in the feature part, which is + 10.0 mV/°C. The relationship between output voltage of the sensor and the centigrade degree at that point can be calculated as follows:

$$T = \frac{(\text{Output Voltage} - 250\times10^{-3}\text{V})}{10\times10^{-3}\text{V}} + 25\,^{\circ}\text{C} \qquad (1)$$

The VEE Pro code shows below.

"meas: volt: dc? (@103)"
Read TEXT xREAL64

The analog input pin for temperature sensor is pin3 (AI@103). It is on read mode.

When the program was started, data from temperature sensor was collected every 0.01 second. The results of output voltage and temperature could be seen in the logging. And the data would be kept in a text file for further diagnostic. The temperature vs. time graph was plotted on the XY chart. After the logic judgment, the warning color will change on the "indicator light" accordingly.

B. Pressure Monitoring

The MPX4250AP sensor output voltage is between 0-5.1V. Also, the relationship between output voltage and absolute pressure is shown in the following graph:

The nominal transfer value is:

$$V_{OUT} = V_S(P\times0.004-0.04)\pm(\text{Pressure Error}\times\text{Temp. Factor}\times0.04\times0.004\times Vs) \qquad (2)$$

$$Vs = 5.1V\pm0.25V_{DC} \qquad (3)$$

The temperature factor is 1 between 0-85 degree and 3 between 85°C to +125°C. And between 20-250kPa, the pressure error is±03.45. The pressure error and temperature factor could be read and calculate from the Figure 9.

Before measuring the pressure of the system, the temperature needs to be known first in order to ensure the range of the temperature factor. And the result must be fed back for the pressure calculation.

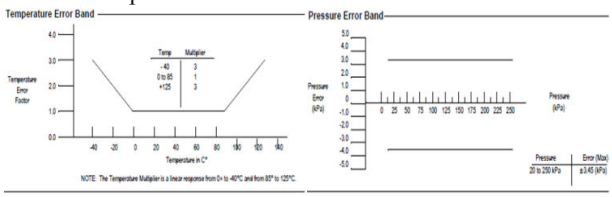

Fig. 9. Temperature and pressure error band

The formulas for the different temperature range are shown below.

$$P = \frac{0.04+\frac{V_{out}+3.45\times1\times0.004\times V_S}{V_S}}{0.004} \quad (0°C \text{ to } +85°C) \qquad (4)$$

$$P = \frac{0.04+\frac{V_{out}+3.45\times3\times0.004\times V_S}{V_S}}{0.004} \quad (85°C \text{ to } +125°C) \qquad (5)$$

The internal system of boiler was a closed-system, so the vapor inside was saturated steam. Therefore, the pressure and temperature measured were also saturated. Saturation pressure and saturation temperature have a direct relationship: saturation temperature increases with the saturation pressure. It can be found in a standard table. If either of the system temperature or pressure was known, the other one was able to be predicted by their relationship. It could be used to check the results in measurement.

C. Rotation Speed Monitoring

The key problem to calculate the rotational speed of the flywheel was the counter design. It was designed and programmed in VEE Pro. It contains two loops: the outer loop was designed to measure certain time period (1s) constantly and the inner loop was designed to read data from speed sensor at short regular interval (every 0.001s). Then by using the number of rounds measured from the inner loop multiple by 60, the rotation speed of flywheel can be calculated with a unit of round per minute.

Since the counter is an accumulator, only the last number which is also the biggest one of every loop needs to be recorded. To solve this problem, within 1 second, all the reading from the sensor were stored into an array by using "collector" function of VEE Pro. Then at the end of the loop, use 'max()' function to pop the last number from array and save in a '.txt' file.

D. Generator

Since the demonstration model has a very low efficiency, the DC motor cannot generate enough electricity to direct

power the LED Array. Hence, the Led Array was connected to the Digital I/O which was controlled by the VEE Pro. It will be programmed to light up according to the output voltage range of DC motor.

The digital I/O pins used in this part were DI/O 501 bit 0,1 and DI/O 502 bit 0 to 7.

Input Voltage	DI/O Pin
0V-0.4V	Bit 0,1 @ 502
0.4V-0.8V	Bit 0-3 @ 502
0.8V-1.2V	Bit0-5 @ 502
1.2V-1.6V	Bit 0-7 @ 502
1.6V-2.0V	Bit 0-7 @ 502 and Bit 0,1 @501

E. Noise Level Monitoring

The following equations show the conversion of sound units (levels), which are used to derive the formula of noise level sensor.

Standard atmospheric pressure (atm) is 101.325kPa

$1\ \text{Pa} = 1\ \text{Pascal} = 1\ \text{N/m}^2$ (6)

$1\ \text{Pa} = 1\ \text{N/m}^2 \equiv 94\ \text{dB SPL}$ (7)

$1\ \text{bar} = 10^5\ \text{Pa}$ (8)

"Sound level" is the sound pressure level in decibel (dB SPL) in this project. The reference sound pressure is:

$p_0 = 20\ \mu\text{Pa} = 2 \times 10^{-5}\ \text{Pa}$ (9)

The reference sound intensity is $I = 10^{-12}\ \text{W/m}^2$ [11] The sound volume (loudness) is determined mostly by the sound pressure p and expressed as sound pressure level Lp in dB.

$$L_p = 20\ \log_{10}\frac{p}{p_0}\ \text{in dB} = L_I = 20\ \log_{10}\frac{I}{I_0}\ \text{in dB} \quad (10)$$

$$p(\text{Pa}) = p_o \times 10^{\frac{L_p\ (\text{dB SPL})}{20}} \quad (11)$$

$$L_I(\text{dB SPL}) = 10 \times \log_{10}\frac{I}{I_0} \quad (12)$$

From the specialization in the data sheet, the nominal sensitivity is -22dB based on 0dB=1.0V/Pa at 1kHz. According to the calculation part, the denominator Pa was taken as the reference sound pressure, 2×10^{-5}Pa. And also, 1 Pa = 1 N/m^2 ≡ 94 dB SPL. Then, the relationship of input and output of the sensor could be conclude as with an input of 94 dB SPL, the output is -22 dB (79.4mV).

F. Combined System

The graphic 'code' of VEE Pro is shown below.

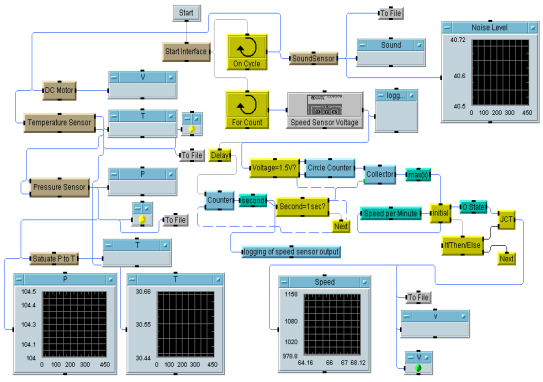

Fig. 10. VEE Pro Programming of combined system

IV. GRAPHIC USER INTERFACE

This graphic user interface is not only for the engineer to monitor the power plant system, but also to do offline plan, control and simulation and provide the following capabilities.

- Monitor the instantaneous output of pressure sensor, temperature sensor, speed sensor, DC generator and noise level sensor
- Collect data and save in .txt file in order to do diagnostic
- Exercise operation, control and monitoring
- Confidential login system
- Alarm system

The major monitoring system is shown below.

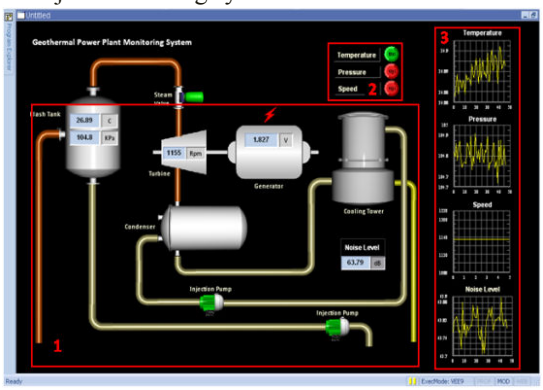

Fig. 11. Major monitoring system

V. TESTING AND DISCUSSION

After finish the circuit connection and monitoring system programming, a testing had been conducted. A group of 1970 numbers of data have been collected from the temperature and pressure sensor. The data were saved to the '.txt' files in computer.

1. Temperature

The initial temperature was 36^{o}C. The maximum temperature which the internal system of boiler can provide was 110.1^{o}C. And the flywheel starts to spin when the temperature hit 105^{o}C.

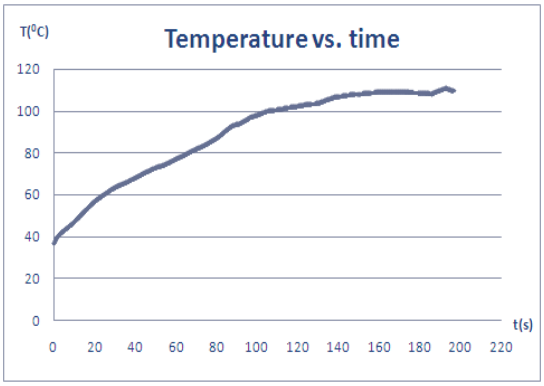

Fig. 12. Temperature vs. time

From the graph, after the temperature of steam reach 100 ^{o}C, the temperature –time relationship appeared to be nonlinear. It is due to the saturated environment inside the boiler. And the relationship of saturated temperature and

pressure can be checked in the standard table.

2. Pressure

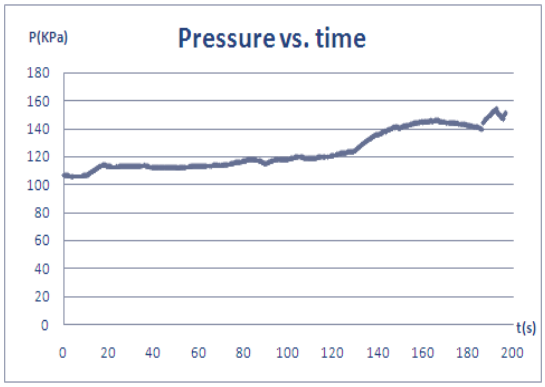

Fig. 13. Pressure vs. time

From the pressure sensor results, the initial pressure was 103 KPa. The maximum pressure which the internal system of boiler can provide was 151.12 kPa. And the flywheel starts to spin when the pressure hit 138 kPa.

There are several twists and turns on the curve. These are due to the unstable of the open-loop system. Because of the fuel provided to the system is not uniform, the quantity of steam generate inside the boiler is also uneven.

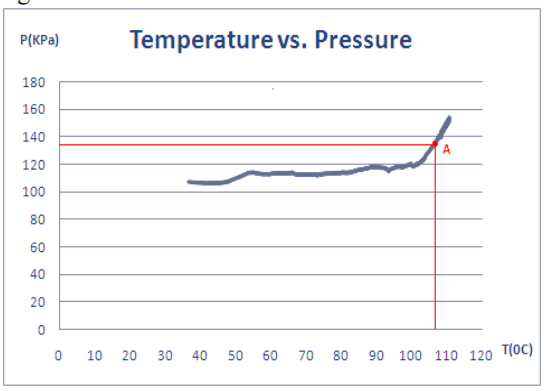

Figure 14. Pressure vs. Temperature

The pressure vs. temperature graph was plotted. A is the point when the flywheel start spinning. At the point, temperature is around 105°C and pressure is 138 kPa.

3. Speed

The speed sensor is a reflective optical sensor. It is mounted in alignment with the flywheel. A black square sticker was stick on the bright surface of flywheel. Since the surface of the flywheel is like a mirror, the black square sticker could be considered as the block object which could absorb the infrared ray. The black square sticker should have a harsh surface finishing; otherwise, it will reflect light and the output voltage differences will not be so obvious. In addition, the edge of black square sticker can be treated as the trigger point when start counting.

Two groups of data have been collected and saved to files. The average speed of 1st group is 375round/min, while the 2nd group is 381.84round/min. Since the fuel of the system could not be provided constantly, the amount of steam is not stable. Thus, the speed of flywheel is not constant either.

The two groups of results was shown in Figure 15.

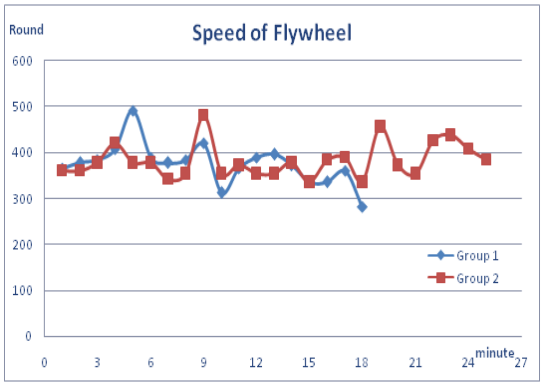

Figure 15. The speed plot of Speed Sensor

4. DC Generator

Thousands of data have been collected, and shown in Figure. 16. The average value of those data is 0.4976v, which means 4 LEDs would be lighten up during the trial run accordingly.

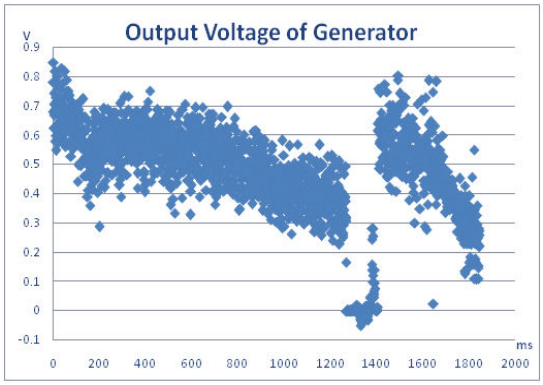

Fig. 16. The results of DC generator output

5. Noise Level

In the relative silent environment, the reading from the sensor was around 40 dB. Use PC to play music and put the sensor 5cm away from the speaker, the reading from the sensor was around 80 dB. The Figure. 17 was drawn by using the readings recorded during a whole song.

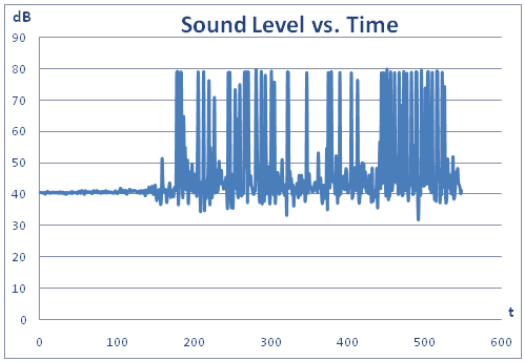

Fig. 17. Sound Level L (loudness) vs. time

VI. CONCLUSION

A geothermal power plant demonstration model and a monitoring graphic user interface were built and tested successfully.

Base on the researches in this project, geothermal power is a reliable and sustainable way to generate electricity. The

technologies to build a efficient geothermal power plant is worth to be popularized. The demonstration model built can give the future researchers an overview of the geothermal power plant in a simpler and easier way. The results obtained in the testing can be used in real-time monitoring or virtual simulation in future research.

ACKNOWLEDGMENT

I would like to thank Agilent Technologies for giving me such a great opportunity of taking part in the final year project competition. I have indeed learnt a lot through the one year project. I also would like to thank Agilent Technologies for the finical supporting on this project.

I would like to take this opportunity to express my deepest gratitude towards my project supervisor, Assistant Professor Koen Mouthaan. He has been so dedicated and helpful in providing guidance for not only this project but also my future academics. Personally I have benefited a lot from his piercing insights and sound methodology for research.

REFERENCES

[1] DiPippo, R., Khalifa, H.E., Correia, R. J. and J. Kestin, "Fossil Superheating in Geothermal Steam Power Plants," Geothermal Energy Magazine, vol. 7, No.1, pp. 17- 23,1979.

[2] Bertani, R. (2009). "Geothermal energy: An overview on resources and potential", International Geothermal Days Slovakia 2009 Conferences & Summer School Session 1: Geothermal Electricity Production: Possibilities, Technical and Economic Feasibility in Central European Region, 2010

[3] Khan, M. A. 2007. The Geysers Geothermal Field, an Injection Success Story. Retrieved 2010, from Annual Forum of the Groundwater Protection Council: http://www.gwpc.org/meetings/forum/2007/proceedings/Papers/Khan,%20Ali%20Paper.pdf

[4] G.W. Hotson and G. Everett., "Energy Model For An Industrial Plant Using Geothermal Steam In New Zealand", Proceedings World Geothermal Congress, pp. 3439- 3445, 2000.

[5] Tester, Jefferson W., "The Future of Geothermal Energy", Impact of Enhanced Geothermal Systems (Egs) on the United States in the 21st Century: An Assessment, pp. 1-8 to 1-33,2006.

[6] Agilent_ Technology. (2000). Agilent VEE Pro 9.0. Retrieved 2009, from Agilent: http://cp.literature.agilent.com/litweb/pdf/5989-9641EN.pdf

[7] Dr. Fullerton., 2006. SoundPLAN Application - Power Plant Noise Survey. Retrieved 12 10, 2009, from Navcon Engineering Network: http://www.navcon.com/splan_powerplant.htm

[8] DiPippo, R., 1980. Geothermal Energy as a Source of Electricity: A Worldwide Survey of the Design and Operation of Geothermal Power Plants USDOE/ RA/ 28320- 1, US Gov. Printing Office, Washington.

[9] "Geothermal Power Systems," R. Dipippo. Sect. 8. 2 in Standard Handbook of Power plant Engineering, 2nd ed., T. C. Elliott, K. Chen and R C. Swanekamp, eds., pp. 8.27 – 8. 60, McGraw- Hill, Inc., New York, 1998.

[10] Oliver, G. J. "Geothermal Energy potential of Singapore", South East Asia Petroleum Exploration society. Second Appointment, 2009.

[11] Tontechnic-Rechner. (n. d.). Tontechnic-Rechner sengpielaudio. Retrieved 2010, from Google: http://www.sengpielaudio.com/calculator-soundlevel.htm

[12] Q. Liu, Y. He, and R. Zhao., "Imitation of the characteristics of the wind turbine based on DC motor", Front. Electr. Electron. Eng. China. No.3. pp. 361–367, 2007

[13] Austin, A. L. and A. W. Lundberg, The LLL Geothermal Energy Program: A Status Report on the Development of the Total Flow Concept, Lawrence Livermore Laboratory Rep. UCRL-50046-77, Livermore, CA.

[14] F. Casella., "Modeling, Simulation, Control, and Optimization of a Geothermal Power Plant", IEEE TRANSACTIONS ON ENERGY CONVERSION, VOL. 19, NO. 1. pp. 170 – 178, 2004

[15] IEEE Criteria for Class IE Electric Systems (Standards style), IEEE Standard 308, 1969.